



# Fabrication of porous bone scaffolds using degradable and mouldable bacterial cellulose

Yunus Emre Öz · Nur Deniz Bingül ·  
Zehra Gül Morçimen · Aylin Şendemir ·  
Elif Esin Hameş

Received: 3 September 2023 / Accepted: 22 January 2024 / Published online: 25 February 2024  
© The Author(s) 2024

**Abstract** Bacterial cellulose (BC) is a biomaterial extensively studied in tissue engineering due to its favorable properties. Porosity, biocompatibility, biodegradability and mechanical durability are essential material properties for scaffold use in tissue engineering. This study aims to fabricate porous scaffolds using a moldable and degradable BC-HAp composite for bone tissue engineering. BC was produced by *Komagataeibacter sucrofermentans* under static culture conditions. The harvested BC membranes were purified and then mechanically shredded. BC oxidation was performed using different sodium periodate concentrations (0.05–0.5 M) and treatment times (0.5–12 h). Oxidized BCs (oxBC) were modified with hydroxyapatite (HAp), then were moulded,

lyophilized, and characterized. The degradability of the scaffolds was determined for 45 days. Cytotoxic analysis of oxBC scaffolds was carried out for 7 days using the L929 fibroblast cell line. The oxidation degrees of the shredded BC samples were between 6.75 and 81%, which increased in line with the increasing concentration and application time of periodate. The scaffolds prepared using oxidized cellulose for 30 and 60 min (oxBC<sub>30</sub> and oxBC<sub>60</sub>) preserved their integrity. These scaffolds showed a weight loss of 9% and 14% in 45 days, respectively. The pore distribution was between 50 and 450 µm and concentrated in the 50–150 µm range. The compression moduli were 88.72 kPa and 138.88 kPa for oxBC<sub>30</sub>-HAp and oxBC<sub>60</sub>-HAp, respectively. It was determined that oxBC did not show a significant difference in cell viability compared to the control groups and was not cytotoxic. In conclusion, degradable and more porous bone scaffolds were fabricated using mouldable oxBC.

Yunus Emre Öz and Nur Deniz Bingül have contributed equally to this work.

Y. E. Öz · N. D. Bingül · Z. G. Morçimen · A. Şendemir ·  
E. E. Hameş  
Department of Bioengineering, Graduate School  
of Natural and Applied Sciences, Ege University,  
35040 Bornova, Izmir, Türkiye

A. Şendemir · E. E. Hameş (✉)  
Department of Bioengineering, Faculty of Engineering,  
Ege University, 35040 Bornova, Izmir, Türkiye  
e-mail: esin.hames@ege.edu.tr; esinhames@gmail.com

A. Şendemir · E. E. Hameş  
Department of Biomedical Technologies, Graduate  
School of Natural and Applied Sciences, Ege University,  
35040 Bornova, Izmir, Türkiye

**Keywords** Bacterial cellulose · Oxidation ·  
Mouldable · Bone scaffolds · Degradation

## Introduction

BC is a highly pure exopolysaccharide that can be produced by some microorganisms (Emre Oz et al. 2021; Hou et al. 2018). It is used in wound dressing, drug delivery systems, biosensors, food supplements,

packaging, electronic devices, cosmetics, and tissue engineering applications (Bingül et al. 2022; Marestoni et al. 2021). Although it has the same molecular formula as plant-derived cellulose, BC is an alternative biomaterial that has been extensively studied in tissue engineering in recent years for its properties such as high purity, high mechanical strength, biocompatibility, high crystallinity, nanofiber structure, porosity, and high water-holding capacity (Emre Oz et al. 2021; Yang et al. 2016). Purity, porosity, biocompatibility, biodegradability, and mechanical strength are important properties of materials used for scaffolds in tissue engineering (Pan et al. 2023). Individual BC chains have robust nanofibril architecture similar to collagen, with a structure much finer than plant cellulose fibres. In addition, since BC does not exhibit any immunological reactivity, it is successfully used in biomedical applications (Manan et al. 2022).

BC has been used in many tissue engineering studies because it can be easily modified in situ or ex situ (Emre Oz et al. 2021). However, it is not biodegradable, or its degradability is quite low as no enzymatic reaction in the human body can break the  $\beta$  1–4 glucose bonds of cellulose (Stilwell et al. 1998; Wang et al. 2016a). While non-biodegradable scaffolds help initiate tissue regeneration, they may cause adverse reactions in the long term, and require further patient surgery for removal (Madaghiele et al. 2014). BC can be converted to degradable form by oxidation using periodate, nitrogen dioxide, metaperiodate and hypochlorite (Hou et al. 2018; Solomevich et al. 2020). Among these cellulose chemical modification pathways, only periodate oxidation selectively opens glucose rings. Periodate oxidation cleaves bonds between neighbouring diols and converts primary alcohols to formaldehyde and secondary alcohols to aldehyde groups (Hou et al. 2018; Luz et al. 2020; Peng et al. 2012). This changes the chemical structure of cellulose, and the presence of aldehyde groups increases its reactivity. The presence of aldehyde groups can change the surface chemistry of cellulose, providing better wettability (Isogai et al. 2011). These aldehyde groups can form chemical bonds with other reactive molecules. This allows cellulose to be modified easier with other materials. Aldehyde groups can form bonds with polymers bearing amine groups (Mudedla et al. 2021; Zhang et al. 2018; Hou et al. 2018).

Bone tissue engineering applications offer alternatives for treating bone disorders due to the increasing elderly population, obesity, and poor physical activity (Amini et al. 2012). Hydroxyapatite (HAp), which is chemically similar to inorganic bone matrix components and can bind to human tissues, is frequently used in bone tissue engineering research (Amini et al. 2012; Zhou and Lee 2011). HAp is a highly biologically active, osteoconductive, and biocompatible calcium phosphate (Sathiyavimal et al. 2020). In addition, HAp, which has a brittle structure and low bending strength, can be used as an additive to various polymers such as BC, chitosan, and collagen, making it suitable for bone tissue engineering (Bayır et al. 2019; Kane et al. 2015; Wilson and Hull 2008).

This study aimed to fabricate bone scaffolds with increased pore diameter using degradable BC in mouldable form. With shredded BC membranes, degradability and HAp modification were achieved homogeneously, and then the production of scaffolds in the desired thickness and shape was realized thanks to mouldability.

## Materials and methods

### Cultivation of microorganisms

Cultivation of *Komagataeibacter sucrofermentans* ATCC 700178 (formerly known as *Gluconacetobacter xylinus*) was carried out for 24–48 h at 30 °C in agitated (150 rpm) culture in Hestrin & Schramm (HS) medium with an initial pH of 5.5, containing 2.5 D(+) glucose (% w/v) (Merck, 50–99-7, Germany), 0.5 (% w/v) bacteriological peptone (LabM, MC024, UK), 0.5 (% w/v) yeast extract (Merck, 8013–01-2, USA), 0.27 (% w/v) Na<sub>2</sub>HPO<sub>4</sub>·2H<sub>2</sub>O (Merck, 1028–24-7, Germany) and 0.115 (% w/v) citric acid monohydrate (Merck, 5949–29-1, Germany) (Hestrin and Schramm 1954).

### BC production, purification, and shredding

In BC production, active culture was inoculated (2% v/v) into HS medium in at least triplicate and incubated at 30 °C for seven days under static culture conditions. The harvested BC membranes were rinsed in distilled water to remove the medium and bacterial residues, and then purified with a slightly

modified alkaline purification method (Bilgi et al. 2016). For this, BC samples were boiled in 0.1 M NaOH (Merck, 106,462, USA) for one hour (If the BC membrane did not whiten, the procedure was repeated). Afterwards, the samples were placed in fresh distilled water and boiled thrice for total of 20 min. BC samples were then boiled in ultrapure water for 10 min and mechanically shredded by a blender (10,000 rpm, 10 min). Finally, the pellets were filtered to remove free water after shredding, then centrifuged at 6000 rpm for 15 min, and BC pellets were stored at 4 °C until use.

### BC oxidation

BC oxidation was carried out with sodium periodate ( $\text{NaIO}_4$ ), according to Hou et al. (2018). Preliminary test results of scaffolds fabricated using BC samples oxidized by different concentrations (0.05–0.5 M) of sodium periodate for different durations (0.5–12 h) showed that the integrity of the scaffold was preserved when sodium periodate at 0.05 M concentration was used. Therefore, optimization of application time was carried out in triplicate using 0.05 M of sodium periodate for 30, 60, 90, 180, and 360 min at 40 °C in the dark, under agitated conditions. Then, the oxidation reaction was stopped by 1% (v/v) ethylene glycol, and the oxidized BC (oxBC) samples were washed three times by distilled water to remove sodium periodate. Then, as in the shredding process, the free water of the BC pellet was removed by filtration and centrifugation.

### HAp modification of oxBC

Hydroxyapatite (HAp) modification was performed according to Huang et al. (2017). Oxidized and unoxidized shredded BC samples were incubated in 0.1 M  $\text{CaCl}_2$  in triplicate at 37 °C for three days, and the  $\text{CaCl}_2$  solution was changed daily. Next, the samples were washed three times with distilled water, transferred to 1.5× simulated body fluid (SBF) (Sasikumar et al. 2017) and incubated at 37 °C for seven days, changing SBF daily. After that, the samples were washed three times with ultrapure water and filtered, and then the BC pellets were separated by centrifugation at 6000 rpm for 15 min.

### Scaffold production

Our preliminary studies showed that the scaffold's porosity fabricated with BC pellets, which were degraded and their free water was removed, increased compared to the BC membranes. When BC pellets were diluted with distilled water, the scaffolds failed to retain their shape after freeze-drying and rapidly dispersed in water. For these reasons, this study used fragmented, oxidized, HAp-modified BC pellets directly in scaffold production without dilution. For this 0.2 g of wet BC pellets were transferred to a 96-well plate (0.4 g and 48 well plate for mechanical characterization) and freeze-dried.

### Characterization of oxBC

#### *Oxidation degree*

Oxidation degrees of the samples were determined in triplicate by the Cannizzaro method. Specifically, 0.1 g of BC sample was incubated with 20 mL of 0.05 M NaOH at 70 °C for 25 min with stirring, then the suspension was cooled to room temperature, and 10 mL of 0.1 M HCl (Carlo Erba 302,626) was added. Finally, excess acid was titrated with 0.1 M NaOH until the pH of the solution became neutral pH, and the oxidation degree (OD) was determined with the following Eq. (1) (Hou et al. 2018).

$$OD = ((V1 - V2) \times N \times 162 / M) \times 100 / 2 \quad (1)$$

where  $V1$  is the amount (L) of NaOH used for titration in the cellulose sample,  $V2$  is the amount (L) of NaOH used for titration in the cellulose-free sample,  $N$  is the NaOH concentration used for titration, and  $M$  is the weight (g) of oxidized cellulose.

#### *Water holding capacity*

The water holding capacity was determined by dividing the mass of removed water by the dry weight of BC (Schrecker and Gostomski 2005). For this, 3 one-gram oxidized BC samples were dried at 70 °C until their weight did not change, and the water-holding capacity was calculated according to the following Eq. (2).

$$\text{Water holding capacity} = (WW - DW) / DW \quad (2)$$

$WW$  is the wet weight of BC (g), and  $DW$  is the dry weight of BC (g).

#### Fourier transform infrared spectroscopy (FTIR)

FTIR spectroscopy provides structural, compositional, and functional information arising from vibrations of the bonds and functional groups of the samples. FTIR analyses of scaffolds were performed with a resolution of  $4\text{ cm}^{-1}$  in the band range of  $400\text{--}4500\text{ cm}^{-1}$  (Jasim et al. 2017).

#### Scanning electron microscopy (SEM)

SEM analysis of the samples was performed to determine the surface morphology of oxBC, examine the effect of oxidation on BC and determine the pore sizes of moulded BC. Lyophilized samples were coated with gold–palladium of about 8 nm thickness. SEM–EDS (Energy dispersive spectrometry) analysis was performed to determine the surface components of the scaffold. SEM (Thermo Scientific Apreo S device) in Ege University Central Research, Test and Analysis Laboratories was used.

#### Mechanical characterization

Bone tissue scaffold samples of 10.7 mm diameter, 10 mm height were subjected to a static compression test with a Dynamic Mechanical Analysis (DMA Q800) device to determine the mechanical compression moduli after freeze-drying. The analysis was performed at  $37^\circ\text{C}$ , and 1 N/min loading rate in Ege University Central Research, Test and Analysis Laboratories. The moduli were calculated from the slope of the elastic range of stress–strain curves.

#### In vitro degradability test

The degradability of oxBC-HAp scaffolds was determined in phosphate-buffered saline (PBS) (pH 7.4) at  $37^\circ\text{C}$  for 45 days in static conditions. Samples were weighed and placed in PBS, and the solution was refreshed daily throughout the test. Samples taken at 4, 8, 12, 24, 72, 168, 360, 504, 720, and 1080 h were washed with distilled water, lyophilized, weighed, and the degradation was determined using the Eq. (3) given below (Li et al. 2009). All measurements were done in 3 repetitions.

$$\text{Degradation} = (C_0 - C)/C \times 100 \quad (3)$$

where  $C_0$  is the initial weight, and  $C$  is the final weight.

#### In vitro cell viability

Mouse fibroblast cells (L929) (ATCC) is one of the cell lines recommended by ISO 10993–12 standard for cytotoxicity testing, which is suitable to represent the mammalian system. L929 cells were cultured in high glucose Dulbecco's Modified Eagle's Medium (DMEM) (Capricorn) containing 10% heat-inactivated fetal bovine serum (FBS) (Capricorn), 1% L-glutamine (Capricorn) and 100  $\mu\text{U}/\text{mL}$  penicillin/streptomycin (Capricorn) culture medium at  $37^\circ\text{C}$  in 5%  $\text{CO}_2$  atmosphere incubator.

Ethylene oxide was used to sterilize the scaffolds of 5 mm diameter, 7 mm height; then, they were incubated in a cell culture medium overnight for conditioning. Cells were seeded in triplicate in sterilized and conditioned scaffolds at a concentration of  $10^5$  cells/mL, and cultured in 48-well culture plates in complete culture medium at  $37^\circ\text{C}$  in a  $\text{CO}_2$  incubator. Cell viability on days 1, 4, and 7 was analyzed by AlamarBlue assay.

For AlamarBlue analysis, a serum-free medium containing 10% dye solution (10x) was prepared and homogenized. The medium on the scaffolds was removed, and the medium containing 300  $\mu\text{L}$  of dye was added. Cells were incubated for 4 h at  $37^\circ\text{C}$  in a  $\text{CO}_2$  incubator. After the incubation, 100  $\mu\text{L}$  samples taken from the dyed medium were transferred to a 96-well spectrophotometric reading plate. The absorbance of the samples was measured in a spectrophotometer at wavelengths of 570 and 600 nm. Unoxidized BC scaffolds were used as control.

#### Statistical analysis

Statistical analyses were performed using GraphPad Prism 10 (GraphPad Software, USA). All quantitative experiments were performed in triplicate. Data represent mean values with standard deviations. Statistically significant differences ( $p < 0.05$ ) in the samples were assessed by Dunnett's multiple comparison test.

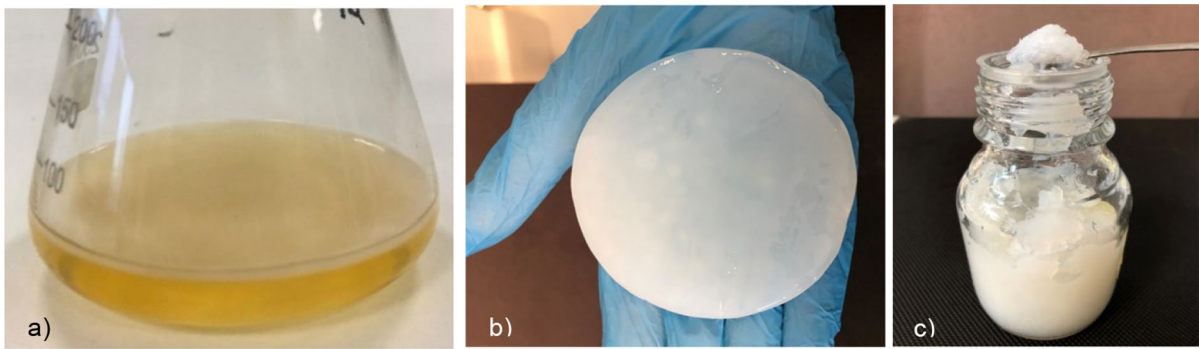


**Fig. 1** **a** BC membrane production in static culture, **b** Appearance of purified BC membrane, **c** BC that is shredded and free water removed (Scale bar = 2 cm). A homogenous pellet structure was observed in the shredded samples

## Results

### BC production, purification and shredding

BC membranes were produced at the liquid–air interface in static culture. After the purification, white semi-opaque BC membranes were mechanically shredded, and free water was removed (Fig. 1).

### BC oxidation

The oxidation degree of the samples increased in parallel with the increasing sodium periodate concentration and the treatment time. The degree of oxidation ( $p < 0.0001$ ) varied widely, from 6.75 to 81% (Fig. 1). It was observed that scaffolds fabricated using oxBC samples with higher oxidation degrees could not maintain their integrity in water and disintegrated. Thus, it was concluded that in optimizing the BC oxidation degree, the oxidation level should be at a level that does not compromise the integrity of the scaffold. For this reason, not only achieving high oxidation but also preserving the integrity of the scaffolds was considered (Fig. 2).

Therefore, oxidation was performed again by applying the lowest concentration of sodium periodate (0.05 M) for shorter treatment times (30–360 min). The scaffolds were named by the time period they were exposed to treatment, e.g. oxBC<sub>60</sub> denoting the scaffold oxidized for 60 min. The oxidation degree of BC samples exposed to oxidation in five time periods varied between 2.81 and 8.31% ( $p < 0.0001$ ) (Fig. 3). Then, each

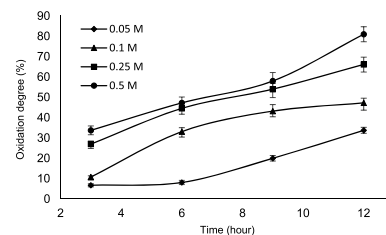


**Fig. 2** Effect of sodium periodate concentration and treatment time on the oxidation degree of BC ( $n = 3$ )

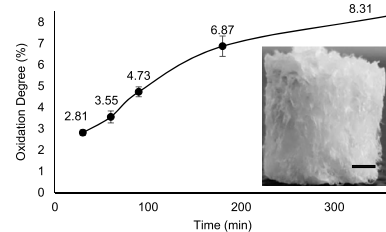


**Fig. 3** Oxidation degree of BC samples (0.05 M NaIO<sub>4</sub>) ( $n = 3$ ) and the appearance of the scaffolds fabricated with oxBC<sub>30</sub> (Scale bar = 1 mm)

sample ( $n = 3$ ) was transferred (wet weight = 0.2 g, dry weight = 4.52 mg) to a 96-well plate and lyophilized.

### FTIR analysis

In the FTIR plot of the BC scaffolds (Fig. 4), the hydroxyl group corresponds to the stretching

vibration frequency in the  $3400\text{ cm}^{-1}$  band for both HAp and BC. BC appears to have a typical peak at a wavelength of about  $2900\text{ cm}^{-1}$ , corresponding to the absorption spectrum of the C-H bond of cellulose type I. Correlation data shows peak formation is observed for the asymmetric deformation vibration of methyl and methylene in the  $1430\text{ cm}^{-1}$  band of the BC scaffold and the  $\text{CH}_2$  bending vibration in the  $1367\text{ cm}^{-1}$  band. In the BC-HAp scaffold, the two weak bands at  $1420\text{ cm}^{-1}$  and  $875\text{ cm}^{-1}$  correspond to the stretching mode of  $\text{CO}_3^{2-}$  ions. The peaks in the  $1730\text{--}1741$  ( $1730$  for  $\text{oxBC}_{30}$ ,  $1735$  for  $\text{oxBC}_{90}$  and  $\text{oxBC}_{180}$  and  $1741$  for  $\text{oxBC}_{60}$ ) and  $880\text{ cm}^{-1}$  bands in the oxidized scaffolds indicate the motion in the C=O stretching mode and the formation of hemiacetal bonds between the newly obtained aldehyde and the hydrated groups.

#### In vitro degradation of oxBC scaffolds

The degradation experiment was completed with scaffolds fabricated with oxidized BC for 30 and 60 min ( $\text{oxBC}_{30}$  and  $\text{oxBC}_{60}$ ). BC scaffolds exposed to longer oxidation times (90, 180 and 360 min) lost their integrity before the end of the degradation experiment (Fig. 5a). The degradability of  $\text{oxBC}_{30}$  and  $\text{oxBC}_{60}$  scaffolds was 9% and 14%, respectively,

after 45 days in phosphate-buffered saline (Fig. 5b). Specifically, the scaffolds produced  $\text{oxBC}_{90}$  lost their integrity on the 21st day, whereas the scaffolds  $\text{oxBC}_{180}$  and  $\text{oxBC}_{360}$  lost their integrity on the seventh day.

#### SEM analysis

Biomimetic HAp synthesis was performed on oxidized BC fibres, then moulded and lyophilized. SEM images of the scaffolds fabricated using BCs exposed to four different oxidation times showed that they were similar to each other and similar to those fabricated with unoxidized BC. Figure 6(a–e) shows the porous structure of the 3D  $\text{oxBC}$ -HAp scaffold, and Fig. 6f and g show HAp crystals synthesized on BC fibres and the Ca content of the crystals, respectively. Elemental composition analysis of EDX results indicate that the precipitated crystals have an approximate Ca/P elemental ratio of 1.6, which is close to the stoichiometric ratio of bone HAp (1.67).

Figure 7 shows the pore size distribution of the scaffolds fabricated by moulding and lyophilizing the shredded BC. It is seen that the pore diameter of the scaffolds is distributed in the range of  $50\text{--}450\text{ }\mu\text{m}$ . Additionally, it was determined that the pore diameter distribution in the scaffolds produced with unoxidized BC was relatively lower ( $p < 0.001$  and  $p < 0.0001$ ).

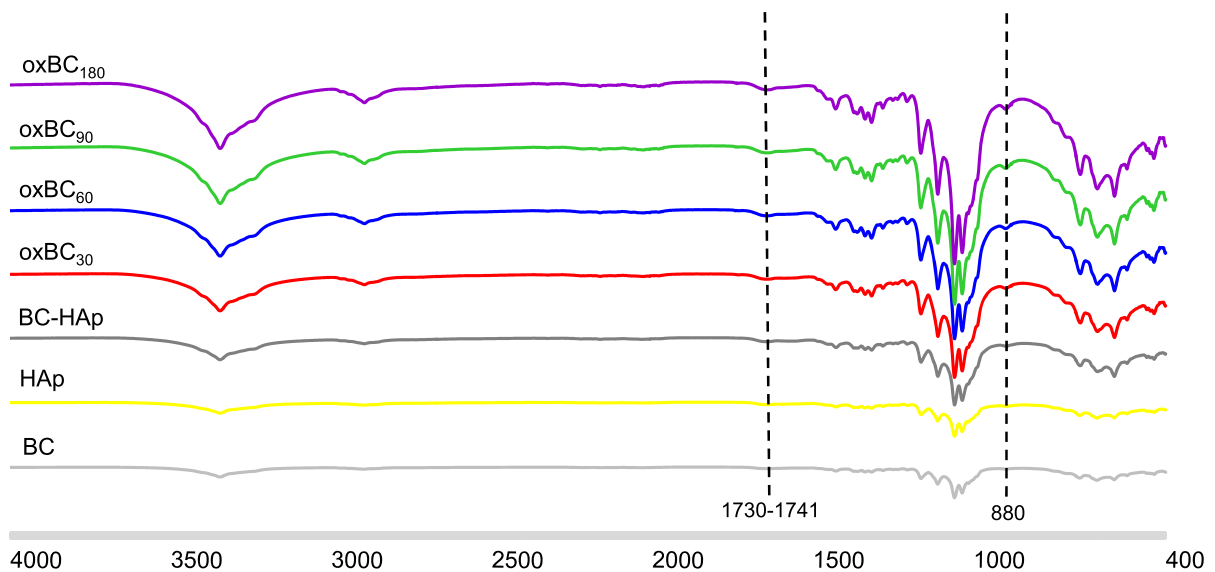


**Fig. 4** FTIR spectrum of the samples

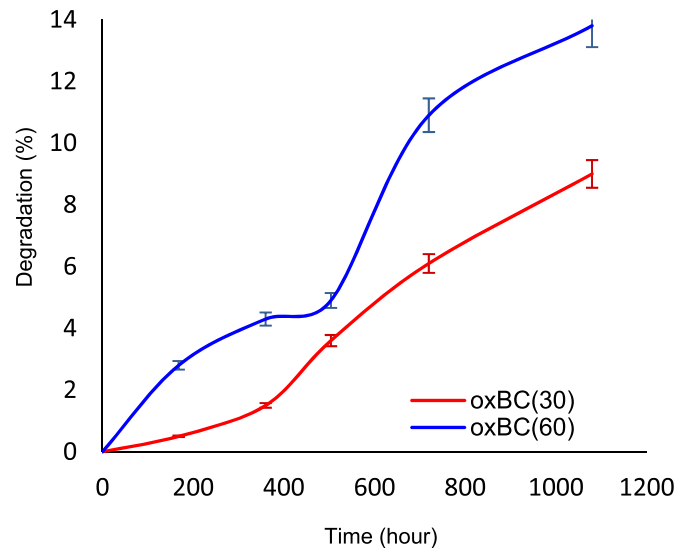
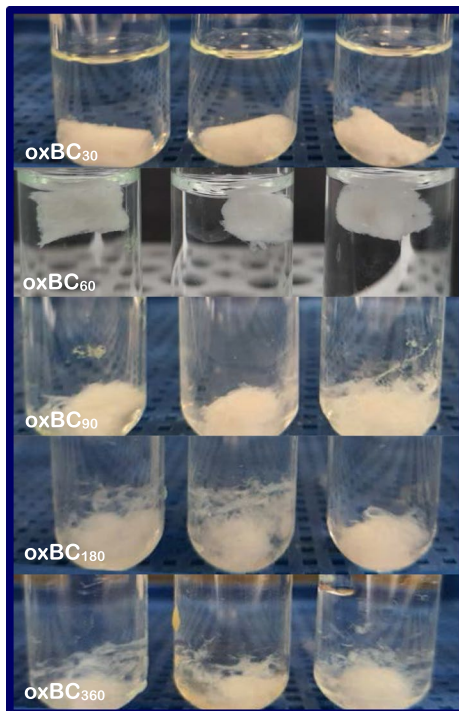


**Fig. 5** **a** Appearance of scaffolds ( $n=3$ ) fabricated with BC exposed to different oxidation times (30–360 min) on the 45th day, **b** Mass loss of oxBC<sub>30</sub> and oxBC<sub>60</sub> scaffolds ( $n=3$ ) (Scale bar=2 mm)

than that of oxidized ones. However, it was determined that increasing oxidation times did not have a significant effect on pore diameter formation.

#### Mechanical characterization

The mechanical compression test results for of BC, BC-HAp, oxBC<sub>30</sub>, oxBC<sub>60</sub>, oxBC<sub>30</sub>-HAp and oxBC<sub>60</sub>-HAp tissue scaffolds are shown in Fig. 8. Compression modulus values were calculated as 190 kPa, 840 kPa, 265 kPa, 312.5 kPa, 745 kPa, and, 865 kPa for BC, BC-HAp oxBC<sub>30</sub>, oxBC<sub>60</sub>, oxBC<sub>30</sub>-HAp and oxBC<sub>60</sub>-HAp, respectively. There was a significant increase in the compression moduli of the scaffolds when HAp precipitation was applied. There was also a more modest increase in the compression moduli with oxidation.

#### Cell viability on oxBC-HAp scaffolds

It was determined that there was no statistically significant difference between oxBC scaffolds and control BC scaffolds in terms of cell viability (Fig. 9).

Also, it is seen that the increase in cell viability on the 4th and 7th days between the groups also showed a similar trend, indicating that there is no cytotoxicity due to oxidation of BC.

#### Discussion

BC, with its unique properties that increase cell adhesion and promote cell proliferation, migration and subsequent differentiation (Swingler et al. 2021), has been improved with varied components and methods in scaffolding studies in recent years. Since BC is produced at the liquid–air interface in static culture, its size and shape (round, square, triangle) take the form of the culture container (Leitao et al. 2016). However, studies show that the thickness is increased by extending the incubation time or the pore size and porosity is increased by adding agar pieces or paraffin to the medium (Bayır et al. 2019; Yin et al. 2015). Additionally, various studies are being carried out to increase its degradability, but it does not seem easy to provide all these features together. In this study,

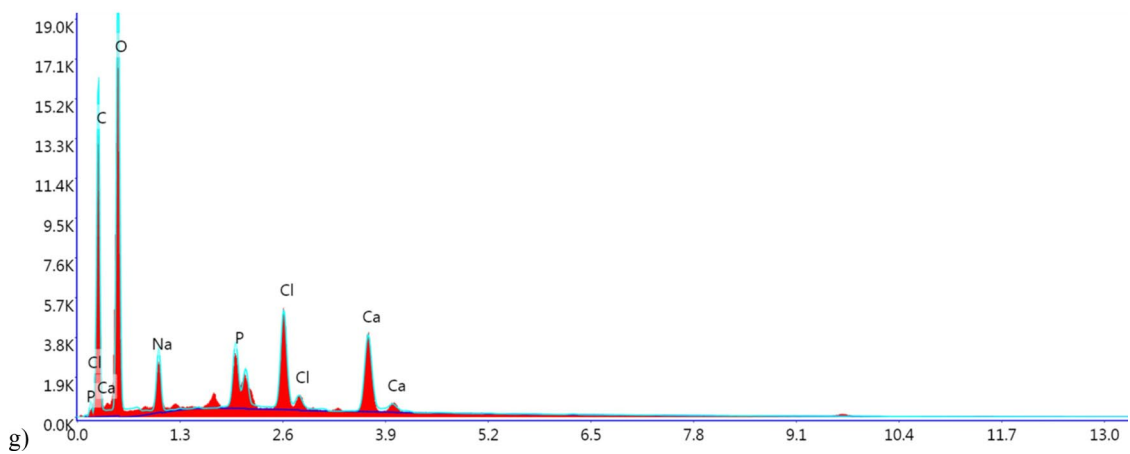
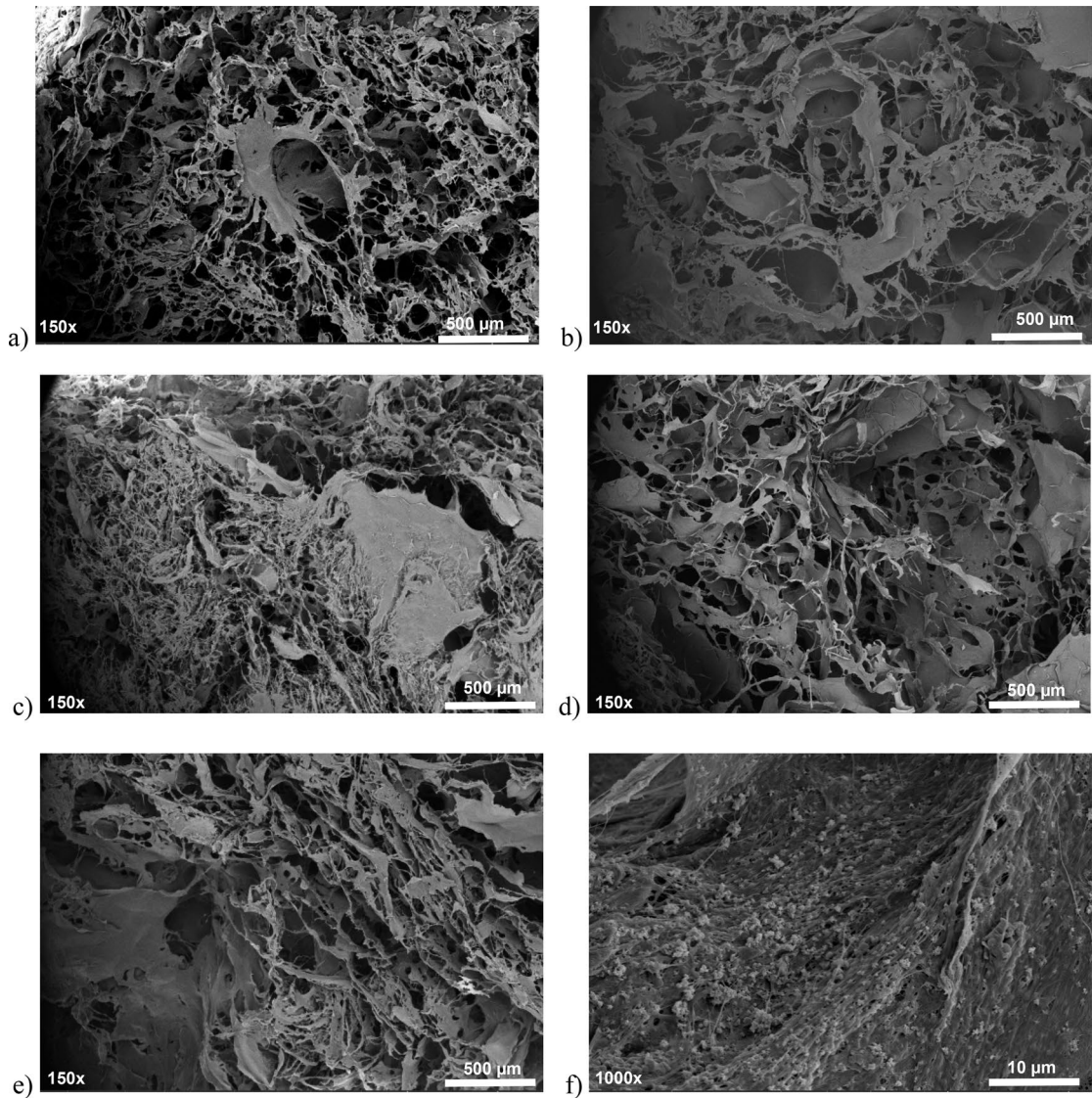




**Fig. 6** The porous structure of oxBC-HAp scaffolds **a** oxBC<sub>30</sub>-HAp, **b** oxBC<sub>60</sub>-HAp, **c** oxBC<sub>90</sub>-HAp, **d** oxBC<sub>180</sub>-HAp **e** unoxidized BC scaffold, **f** Hydroxyapatite crystals on the oxBC-HAp scaffold, **g** SEM–EDS results of HAp crystals

the hypothesis that a more degradable, porous BC scaffold of the desired shape and size for bone tissue engineering can be produced by post-fragmented oxidation and HAp synthesis followed by moulding was investigated. For this purpose, BC produced as a membrane was mechanically fragmented, its oxidation was optimized with sodium periodate, HAp precipitation onto BC was carried out, and finally, it was placed in moulds and freeze-dried.

Periodate oxidation aims to convert 1,2-dihydroxy groups to dialdehyde and is often used in the structural analysis of carbohydrates and derivatization of polysaccharides. When this reaction is applied to 1,4-glucans, it cleaves the C2–C3 bond in the glucopyranose ring, and the emerging hydroxyl groups are then oxidized to dialdehyde. It has been reported that dialdehyde-containing cellulose can be degraded by hydrolysis under physiological conditions (Hou et al. 2018). Cellulose, which has a high dialdehyde content, can become biodegradable by hydrolysis (Li et al. 2009). In addition to more homogeneous HAp synthesis on BC by the fragmentation of BC, BC oxidation can also improve the ability of BC to form composites with different polymers, including HAp. The oxidation degree of BC oxidized with sodium periodate were measured between 6.75 and 81%. The high degree of oxidation accelerates the degradation time of the scaffold. Hou et al. (2018) reported high degradation in short periods (about 50% in 7 days) at high oxidation degrees using a BC membrane with tight nanofibers (Hou et al. 2018). In this study, in addition to achieving more homogeneous oxidation using fragmented BC, it was also essential to maintain the integrity of the moulded scaffolds. However, this also allowed the production of a more porous BC scaffold. Results showed that oxidant concentration and oxidation time are critical parameters for producing BC-based scaffolds that maintain their integrity.

On the other hand, a particular time is required for the cells to adhere to the scaffolds, differentiate and form integrity with the tissue. In addition, conditions such as nutrition, age, gender and diseases affect the healing process in humans (Tajvar et al. 2023). For these reasons, it may be possible to choose scaffolds

that maintain their integrity but have a longer degradation time. Alternatively, it seems possible to produce scaffolds that maintain their integrity and have a shorter degradation time by modification of more oxidized BC with different polymers.

BC contains many polar hydroxyl groups (-OH). Therefore, molecular chains interact with intramolecular and intermolecular hydrogen bonds (Maréchal and Chanzy 2000). In the FTIR spectrum, the band at 1055 cm<sup>-1</sup> represents the sugar ring's C–O–C and C–O–H stretching vibrations (Nelson et al. 1964; Park et al. 2003). 1420 cm<sup>-1</sup> and 875 cm<sup>-1</sup> peaks indicate that the PO<sub>4</sub> regions of the HAp structure are partially replaced by carbonate ions (Wan et al. 2007). The peaks of 1097 cm<sup>-1</sup>, 1041 cm<sup>-1</sup>, 957 cm<sup>-1</sup>, 604 cm<sup>-1</sup> and 565 cm<sup>-1</sup> correspond to the P–O stretching mode, indicating the presence of HAp (Wan et al. 2011). 1740 and 880 cm<sup>-1</sup> peaks mean that the C2–C3 bond of the glucopyranoside ring of BC is cleaved, and two aldehyde groups are formed per glucose during oxidation (Hou et al. 2018; Kim et al. 2004). Furthermore, it is seen that the size of these peaks increases in proportion to the increase in the oxidation time.

BC is not biodegradable in the human body as there is no cellulase to hydrolyze cellulose (Wang et al. 2016b). In this study, as expected, no degradation was detected in the scaffolds produced using unoxidized BC. However, BC scaffolds with 30 and 60 min oxidation time using 0.05 M sodium periodate preserved their integrity and showed 9% and 13.8% degradation on the 45th day, respectively (Fig. 5). Therefore, oxBC<sub>30</sub> and oxBC<sub>60</sub> scaffolds were used for further testing.

In tissue engineering, scaffolds are generally fabricated by combining different materials. Because a single material cannot adequately provide cell adhesion, proliferation and differentiation, as well as the mechanical properties expected from a scaffold. BC provides adhesion and living space to cells thanks to its three-dimensional nanofiber network structure. The high surface area of nanofibers can provide better adhesion of cells. In addition, nanofibers' rough or micropatterned surfaces can help cells find more spots for attachment, thereby creating a suitable environment for cells to grow and spread (Yan et al. 2011). However, it has properties that need to be improved, such as pore structure, degradability and similarity to the extracellular cell matrix. Various materials such as PVA (Aki et al. 2020), collagen

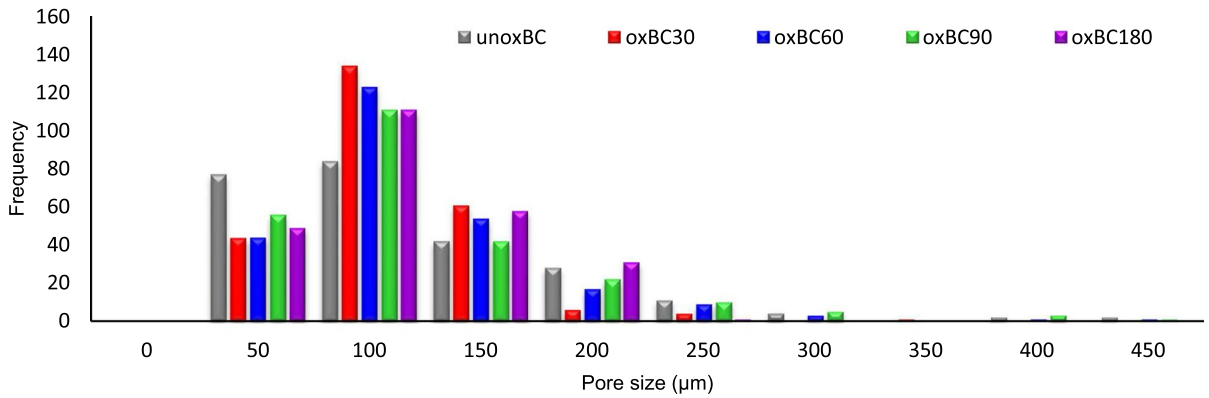


**Fig. 7** Pore size distribution histogram of oxBC scaffolds (250 pores from 5 SEM images for each sample)

**Fig. 8** Compression moduli of BC, BC-HAp, oxBC<sub>30</sub>, oxBC<sub>60</sub>, oxBC<sub>30</sub>-HAp and oxBC<sub>60</sub>-HAp

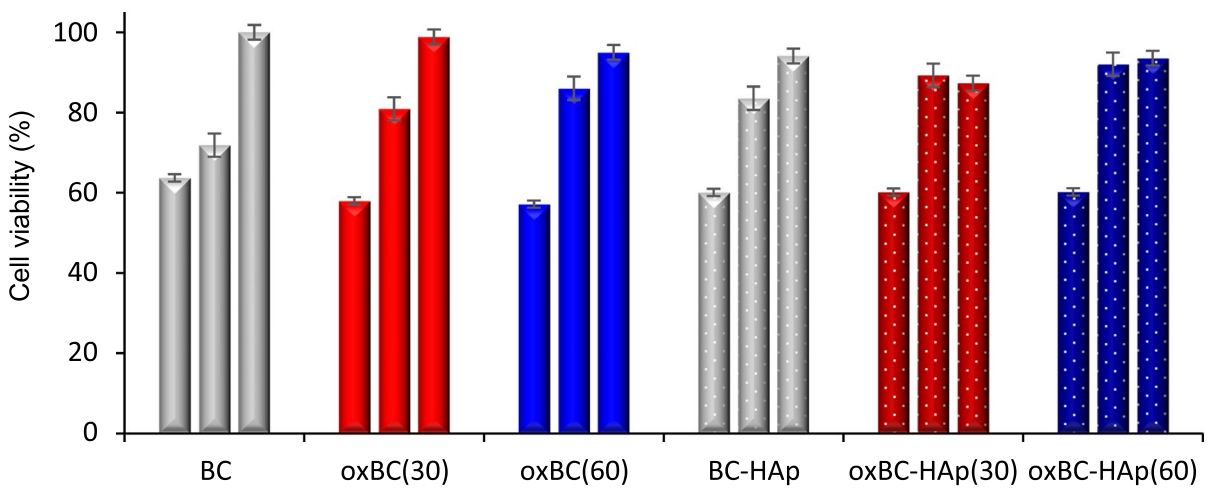
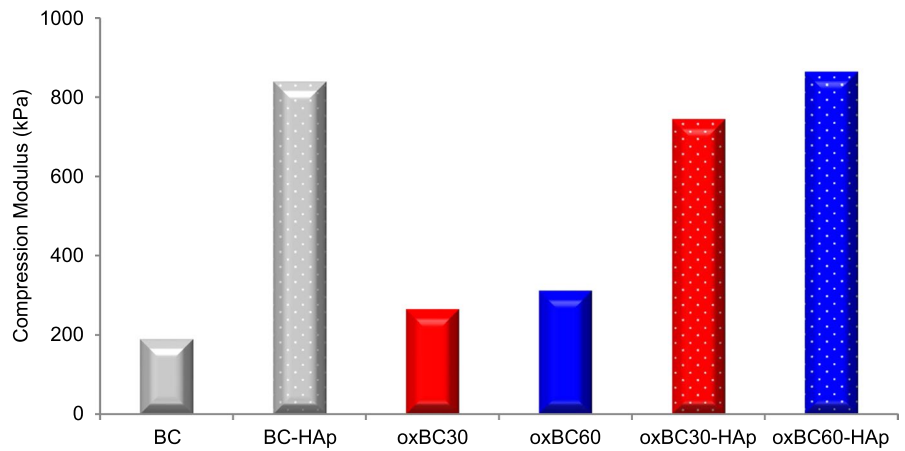


**Fig. 9** Cell viability of L929 cells on BC scaffolds (Days 1, 4 and 7). ( $n = 3$ )

(Saska et al. 2012), chitosan (Zhu et al. 2023), PLA/PEG (Ghalia et al. 2017) and HAp are used in bone tissue engineering studies with BC. As a result of modifications with these materials, better cell proliferation and differentiation results expected from the scaffold can be achieved. In this study, an attempt was made to develop a scaffolding material that is more porous, degradable and flexible. The results showed that high oxidation degrees prevented the BC scaffold from maintaining its integrity.

Degradable oxBC can further be modified by adding different polymers to maintain its integrity. Thus, BC-based materials with higher degradability can be developed. Since BC naturally has a nanofiber structure, it provides an advantage for cell attachment. In addition, thanks to the -OH groups on its surface, BC also allows the synthesis of nanoparticles (Hutchens et al. 2006). Biomimetic HAp synthesis using fragmented BC provided more homogeneous HAp synthesis than membrane BC. During the synthesis of biomimetic HAp with fragmented and oxidized BC, a homogeneous and effective HAp formation occurred due to the increased surface area interaction and dialdehyde content. The nano-sized HAp crystals produced on BC fibres and the nanofiber structure of BC will provide an advantage for cell adhesion and differentiation (Yu et al. 2020).

The pore diameters of native BC produced as a membrane under static culture conditions are not large enough for cell migration (Emre Oz et al. 2021). In tissue engineering applications, it is seen that the cells adhere to the BC membrane from the surface and do not penetrate the material. For this reason, studies have been carried out to increase the BC pore diameter using different methods (Bayır et al. 2019; Yin et al. 2015; Zaborowska et al. 2010). In another study, a composite of printable BC with gelatin was produced by maleic acid treatment and its effect on bone tissue regeneration was evaluated *in vitro* (Wang et al. 2023). Osteoblasts average 20–50 microns in diameter (Qiu et al. 2019), and bone marrow-derived mesenchymal stem cells (BMSCs) average 26 microns (Ge et al. 2014). Materials with pore sizes of 20–1500 microns are used in bone tissue engineering studies (Murphy and O'Brien 2010). However, the literature has stated that the minimum pore size for bone growth should be 75–100  $\mu\text{m}$ . It has been reported that pores larger than 300 microns increase vascularization and bone growth, while pores smaller

than 300 microns increase ossification (formation of bone tissue) (Murphy and O'Brien 2010). It is seen that the pore sizes in oxBC scaffolds are distributed in the range of 50–450  $\mu\text{m}$  (Fig. 6). It can be said that the pore size distribution of oxBC-fabricated scaffolds can support ossification, vascularization and bone growth for osteoblasts and BMSCs.

Most bone scaffolds cannot meet the required mechanical properties (Zhao et al. 2018). In cancellous bones, Young's modulus is relatively high (0.1–2 GPa), while the compressive modulus has lower values (2–20 MPa) (Olszta et al. 2007). In case of minor damage to the bone, a scaffold that is not in the range of 2–20 MPa, with the help of surrounding tissues, may not cause any problems in tissue healing. BC may exhibit different properties depending on the medium and the producer microorganism. The mechanical properties of BC, reported with different compression modulus values in the literature, can be improved with various modifications. A compression modulus of approximately 12 kPa for membranous BC and approximately 20 kPa for spongy BC scaffold formed with gelatin and HAp has been reported (Zhao et al. 2017). In this study, while the compression modulus was 190 kPa for BC, it was calculated as 265 kPa for oxBC<sub>30</sub> and 312.5 kPa for oxBC<sub>60</sub>, increasing in direct proportion to the oxidation time in oxidized samples. This increase in modulus is attributable to increased number of sites for cross-linking on the cellulose fibrils due to oxidation (Syverud et al. 2015). A more pronounced increase was determined in the HAp-containing scaffolds (745 kPa for oxBC<sub>30</sub>-HAp and 865 kPa for oxBC<sub>60</sub>-HAp), as the presence of HAp further increased the compressive modulus (Fig. 8). HAp reinforcement is commonly applied for over 30 years to bone tissue engineering scaffolds as an osteoconductive composite filler to improve mechanical properties (Sasaki et al. 1989; Kane and Roeder 2012). The use of shredded BC for oxidation and HAp precipitation is effective. Compression moduli of scaffolds increased after biomimetic HAp precipitation was applied on these samples. The mechanical properties of oxBC scaffolds (oxBC<sub>30</sub>-HAp and oxBC<sub>60</sub>-HAp) are considered applicable for cancellous bone tissue engineering. A compressive modulus of articular cartilage typically ranges from 320 to 810 kPa (Pei et al. 2023). Therefore, oxBC<sub>60</sub> scaffolds also have potential to be used for cartilage tissue engineering.

As a result of the cell viability assay, it is seen that oxidation is not toxic to cells when compared to the control groups (Fig. 9). Therefore, it was determined that the bone scaffolds prepared with oxBC<sub>30</sub>-HAp and oxBC<sub>60</sub>-HAp did not harm cell viability, and the cell viability was  $87\% \pm 0,13$  and  $94\% \pm 0,24$ , respectively, on the 7th day. However, oxidation causes changes in the surface properties of cellulose. Therefore, cell viability may be adversely affected in scaffolds produced with BC with high oxidation degrees. In this study, no adverse effects of oxidation on cell viability were observed, as reported in other studies (Hou et al. 2018; Kai and Xuesong 2020; Luz et al. 2022).

## Conclusion

Due to the lack of degradability of BC in the human body and the tight nanofiber network structure not allowing cell migration, various studies are available in the literature to increase the degradability and pore size of BC membranes. However, in situ production of BC membranes with increasing pore size, biodegradable and desired size, shape and thickness seems complicated. In this study, BC membranes were mechanically fragmented to achieve homogeneous oxidation, production flexibility through the moulding process, and increase the pore diameter. This approach performed BC oxidation and biomimetic HAp synthesis more effectively than native membrane BC. However, high oxidation prevented the scaffolds from maintaining their integrity in water. Therefore, maintaining scaffold integrity was determined as a constraint on the degree of oxidation. Apart from this, scaffolds with larger pore diameters than the natural BC membrane can be produced since the BC concentration can be adjusted during the moulding process. However, here too, using low concentrations of BC will be a limitation in maintaining the integrity of the scaffolds. As a result, since oxidation constitutes a limitation in maintaining scaffold integrity, it seems possible that this limitation can be overcome by modification of more oxidized BC with another polymer. Thus, more degradable, moldable BC-based scaffolds with increased porosity can be produced.

**Acknowledgments** The authors thank the Ege University Scientific Research Foundation (Project number:

FOA-2020-21947) for funding this research and Özge SÜER for her special support. Yunus Emre ÖZ and Zehra Gül MORÇİMEN is supported by Council of Higher Education (YÖK) 100/2000 Program.

**Authors contributions** Conception and design: AŞ, YEÖ and EEH, Formal analysis and investigation: YEÖ, NDB and ZGM, Data collection and analysis: YEÖ, NDB and ZGM, Writing—first draft preparation: YEÖ and NDB, Writing—review and editing: EEH and AŞ, Supervision: EEH.

**Funding** Open access funding provided by the Scientific and Technological Research Council of Türkiye (TÜBİTAK). This work was supported by The Scientific Research Foundation of Ege University (Project number: FOA-2020–21947).

**Data availability** Data used and/or analyzed during the study are available from the corresponding author upon reasonable request.

## Declarations

**Competing interests** The authors declare no competing interests.

**Consent for publication** All of the material is owned by the authors, and/or no permissions are required.

**Open Access** This article is licensed under a Creative Commons Attribution 4.0 International License, which permits use, sharing, adaptation, distribution and reproduction in any medium or format, as long as you give appropriate credit to the original author(s) and the source, provide a link to the Creative Commons licence, and indicate if changes were made. The images or other third party material in this article are included in the article's Creative Commons licence, unless indicated otherwise in a credit line to the material. If material is not included in the article's Creative Commons licence and your intended use is not permitted by statutory regulation or exceeds the permitted use, you will need to obtain permission directly from the copyright holder. To view a copy of this licence, visit <http://creativecommons.org/licenses/by/4.0/>.

## References

- Aki D, Ulag S, Unal S, Sengor M, Ekren N, Lin CC, Yilmazer H, Ustundag CB, Kalaskar DM, Gunduz O (2020) 3D printing of PVA/hexagonal boron nitride/bacterial cellulose composite scaffolds for bone tissue engineering. *Mater Des* 196:109094. <https://doi.org/10.1016/j.matdes.2020.109094>
- Amini AR, Laurencin CT, Nukavarapu SP (2012) Bone tissue engineering: recent advances and challenges. *Crit Rev Biomed Eng* 40(5):363–408. <https://doi.org/10.1615/critrevbiomedeng.v40.i5.10>
- Bayır E, Bilgi E, Hameş EE, Şendemir A (2019) Production of hydroxyapatite - bacterial cellulose composite scaffolds

- with enhanced pore diameters for bone tissue engineering applications. *Cellulose* 26:9803–9817. <https://doi.org/10.1007/s10570-019-02763-9>
- Bilgi E, Bayir E, Sendemir-Urkmez A, Hames EE (2016) Optimization of bacterial cellulose production by *Gluconacetobacter xylinus* using carob and haricot bean. *Int J Biol Macromol* 90:2–10. <https://doi.org/10.1016/j.ijbiomac.2016.02.052>
- Bingül ND, Öz YE, Şendemir A, Hameş EE (2022) Microbial biopolymers in articular cartilage tissue engineering. *J Polym Res* 29(8):334. <https://doi.org/10.1007/s10965-022-03178-0>
- Emre Oz Y, Keskin-Erdogan Z, Safa N, Hames EE (2021) A review of functionalized bacterial cellulose for targeted biomedical fields. *J Biomater Appl* 36(4):648–681. <https://doi.org/10.1177/0885328221998033>
- Ge J, Guo L, Wang S, Zhang Y (2014) The size of mesenchymal stem cells is a significant cause of vascular obstructions and stroke. *Stem Cell Rev* 10:295–303. <https://doi.org/10.1007/s12015-013-9492-x>
- Ghalia MA, Dahman Y (2017) Fabrication and enhanced mechanical properties of porous PLA/PEG copolymer reinforced with bacterial cellulose nanofibers for soft tissue engineering applications. *Polym Test* 61:114–131. <https://doi.org/10.1016/j.polymertesting.2017.05.016>
- Hestrin S, Schramm M (1954) Synthesis of cellulose by *Acetobacter xylinum*. 2. Preparation of freeze-dried cells capable of polymerizing glucose to cellulose. *Biochem J* 58(2):345–352
- Hou Y, Wang X, Yang J, Zhu R, Zhang Z, Li Y (2018) Development and biocompatibility evaluation of biodegradable bacterial cellulose as a novel peripheral nerve scaffold. *J Biomed Mater Res Part A* 106(5):1288–1298. <https://doi.org/10.1002/jbm.a.36330>
- Huang Y, Wang J, Yang F, Shao Y, Zhang X, Dai K (2017) Modification and evaluation of micro-nano structured porous bacterial cellulose scaffold for bone tissue engineering. *Mater Sci Eng C* 75:1034–1041. <https://doi.org/10.1016/j.msec.2017.02.174>
- Hutchens SA, Benson RS, Evans BR, O'Neill HM, Rawn CJ (2006) Biomimetic synthesis of calcium-deficient hydroxyapatite in a natural hydrogel. *Biomater* 27(26):4661–4670. <https://doi.org/10.1016/j.biomaterials.2006.04.032>
- Isogai A, Saito T, Fukuzumi H (2011) TEMPO-Oxidized Cellulose Nanofibers. *Nanoscale* 3(1):71–85. <https://doi.org/10.1039/c0nr00583e>
- Jasim A, Ullah MW, Shi Z, Lin X, Yang G (2017) Fabrication of bacterial cellulose/polyaniline/single-walled carbon nanotubes membrane for potential application as biosensor. *Carbohydr Polym* 163:62–69. <https://doi.org/10.1016/j.carbpol.2017.01.056>
- Kai J, Xuesong Z (2020) Preparation, characterization, and cytotoxicity evaluation of zinc oxide–bacterial cellulose–chitosan hydrogels for antibacterial dressing. *Macromol Chem Phys* 221(21):2000257. <https://doi.org/10.1002/macp.202000257>
- Kane RJ, Roeder RK (2012) Effects of hydroxyapatite reinforcement on the architecture and mechanical properties of freeze-dried collagen scaffolds. *J Mech Behav Biomed Mater* 7:41–49. <https://doi.org/10.1016/j.jmbbm.2011.09.010>
- Kane RJ, Weiss-Bilka HE, Meagher MJ, Liu Y, Gargac JA, Niebur GL, Wagner DR, Roeder RK (2015) Hydroxyapatite reinforced collagen scaffolds with improved architecture and mechanical properties. *Acta Biomater* 17:16–25. <https://doi.org/10.1016/j.actbio.2015.01.031>
- Kim UJ, Wada M, Kuga S (2004) Solubilization of dialdehyde cellulose by hot water. *Carbohydr Polym* 56(1):7–10
- Leitao AF, Faria MA, Faustino AMR, Moreira R, Mela P, Loureiro L, Silva I, Gama M (2016) A novel small-caliber bacterial cellulose vascular prosthesis: production, characterization, and preliminary in vivo testing. *Macromol Biosci* 16(1):139–150. <https://doi.org/10.1002/mabi.201500251>
- Li J, Wan Y, Li L, Liang H, Wang J (2009) Preparation and characterization of 2,3-dialdehyde bacterial cellulose for potential biodegradable tissue engineering scaffolds. *Mater Sci Eng C* 29(5):1635–1642. <https://doi.org/10.1016/j.msec.2009.01.006>
- Luz EP, Chaves PH, Vieira LD, Ribeiro SF, de Fátima BM, Andrade FK, Muniz CR, Infantes-Molina A, Rodríguez-Castellón E, de Freitas RM, Vieira RS (2020) In vitro degradability and bioactivity of oxidized bacterial cellulose-hydroxyapatite composites. *Carbohydr Polym* 1(237):116174
- Luz EPCG, de Brito Soares AL, de Souza FFP, Andrade FK, Castro-Silva II, de Freitas RM, Vieira RS (2022) Implantable matrixes of bacterial cellulose and strontium apatite: Preclinical analysis of cytotoxicity and osteoconductivity. *Mater Today Commun* 33:104871. <https://doi.org/10.1016/j.mtcomm.2022.104871>
- Madaghiele M, Salvatore L, Sannino A (2014) 4 Tailoring the pore structure of foam scaffolds for nerve regeneration In: Netti PA. (ed) *Biomedical foams for tissue engineering applications* woodhead publishing, pp 101–108. <https://doi.org/10.1533/9780857097033.1.101>
- Manan S, Ullah MW, Ul-Islam M, Shi Z, Gauthier M, Yang G (2022) Bacterial cellulose: molecular regulation of biosynthesis, supramolecular assembly, and tailored structural and functional properties. *Prog Mater Sci* 129:00972. <https://doi.org/10.1016/j.pmatsci.2022.100972>
- Maréchal Y, Chanzy H (2000) The hydrogen bond network in I(β) cellulose as observed by infrared spectrometry. *J Mol Struct* 523(1–3):183–196. [https://doi.org/10.1016/S0022-2860\(99\)00389-0](https://doi.org/10.1016/S0022-2860(99)00389-0)
- Marestoni LD, Barud HD, Gomes RJ, Catarino RP, Hata NN, Ressutte JB, Spinosa WA (2021) Commercial and potential applications of bacterial cellulose in Brazil: ten years review. *Polímeros*. 7(30):e2020047. <https://doi.org/10.1590/0104-1428.09420>
- Mudedla SK, Vuorte M, Vejjola E, Marjamaa K, Koivula A, Linder MB, Arola S, Sammalkorpi M (2021) Effect of oxidation on cellulose and water structure: a molecular dynamics simulation study. *Cellulose* 28(7):3917–3933. <https://doi.org/10.1007/s10570-021-03751-8>
- Murphy CM, O'Brien FJ (2010) Understanding the effect of mean pore size on cell activity in collagen-glycosaminoglycan scaffolds. *Cell Adh Migr* 4(3):377–381. <https://doi.org/10.4161/cam.4.3.11747>

- Nelson ML, O'Connor RT (1964) Bands, relation of certain infrared bands to cellulose crystallinity and crystal lattice type, Part 1. spectra of lattice types I, II, III and of amorphous cellulose. *J Appl Polym Sci* 8(3):1311–1324. <https://doi.org/10.1002/app.1964.070080322>
- Olszta MJ, Cheng X, Jee SS, Kumar R, Kim Y-Y, Kaufman MJ, Douglas EP, Gower LB (2007) Bone structure and formation: a new perspective. *Mater Sci Eng R Rep* 58(3–5):77–116. <https://doi.org/10.1016/j.mser.2007.05.001>
- Pan X, Li J, Ma N, Ma X, Gao M (2023) Bacterial cellulose hydrogel for sensors. *Chem Eng J* 461:142062. <https://doi.org/10.1016/j.cej.2023.142062>
- Park JK, Park YH, Jung JY (2003) Production of Bacterial Cellulose by Gluconacetobacter Hansenii PJK Isolated from Rotten. *Appl Biotechnol Bioproc E* 8:83–88. <https://doi.org/10.1007/BF02940261>
- Pei W, Yusufu Y, Zhan Y, Wang X, Gan J, Zheng L, Wang P, Zhang K, Huang C (2023) Biosynthesizing lignin dehydrogenation polymer to fabricate hybrid hydrogel composite with hyaluronic acid for cartilage repair. *Adv Compos Hybrid Mater* 6(5):180. <https://doi.org/10.1007/s42114-023-00758-6>
- Peng S, Zheng Y, Wu J, Wu Y, Ma Y, Song W, Xi T (2012) Preparation and characterization of degradable oxidized bacterial cellulose reacted with nitrogen dioxide. *Polym Bull* 68(2):415–423. <https://doi.org/10.1007/s00289-011-0550-8>
- Qiu Z, Cui Y, Wang X (2019) Natural bone tissue and its biomimetic. In: Mineralized collagen bone graft substitutes (Vol. 10). Woodhead Publishing Series in Biomaterials pp 1–22. <https://doi.org/10.1016/B978-0-08-102717-2.00001-1>
- Sasaki N, Umeda H, Okada S, Kojima R, Fukuda A (1989) Mechanical properties of hydroxyapatite-reinforced gelatin as a model system of bone. *Biomaterials* 10(2):129–132. [https://doi.org/10.1016/0142-9612\(89\)90046-X](https://doi.org/10.1016/0142-9612(89)90046-X)
- Sasikumar Y, Solomon MM, Olasunkanmi LO, Ebenso EE (2017) Effect of surface treatment on the bioactivity and electrochemical behavior of magnesium alloys in simulated body fluid. *Mater Corros* 68(7):776–790. <https://doi.org/10.1002/maco.201609317>
- Saska S, Teixeira LN, de Oliveira PT, Gaspar AMM, Ribeiro SJL, Messaddeq Y, Marchetto R (2012) Bacterial cellulose-collagen nanocomposite for bone tissue engineering. *J Mater Chem* 22(41):22102–22112. <https://doi.org/10.1039/C2JM33762B>
- Sathiyavimal S, Vasantharaj S, LewisOscar F, Selvaraj R, Brindhadevi K, Pugazhendhi A (2020) Natural organic and inorganic-hydroxyapatite biopolymer composite for biomedical applications. *Prog Org Coat* 147:105858. <https://doi.org/10.1016/j.porgcoat.2020.105858>
- Schrecker ST, Gostomski PA (2005) Determining the water holding capacity of microbial cellulose. *Biotechnol Lett* 27:1435–1438. <https://doi.org/10.1007/s10529-005-1465-y>
- Solomevich SO, Dmitruk EI, Bychkovsky PM, Nebytov AE, Yurkshovich TL, Golub NV (2020) Fabrication of oxidized bacterial cellulose by nitrogen dioxide in chloroform/cyclohexane as a highly loaded drug carrier for sustained release of cisplatin. *Carbohydr Polym* 248:116745. <https://doi.org/10.1016/j.carbpol.2020.116745>
- Stilwell RL, Marks MG, Saferstein L, Wiseman DM (1998) 15. Oxidized cellulose: chemistry, processing and medical applications. *Drug Target. Recov Handb Biodegrad Polym* 7:291–306
- Swingler S, Gupta A, Gibson H, Kowalczyk M, Heaselgrave W, Radecka I (2021) Recent advances and applications of bacterial cellulose in biomedicine. *Polymers* 13(3):412. <https://doi.org/10.3390/polym13030412>
- Syverud K, Pettersen SR, Draget K, Chinga-Carrasco G (2015) Controlling the elastic modulus of cellulose nanofibril hydrogels-scaffolds with potential in tissue engineering. *Cellulose* 22:473–481
- Tajvar S, Hadjizadeh A, Samandari SS (2023) Scaffold degradation in bone tissue engineering: an overview. *Int Biodeterior Biodeg* 180(May):105599. <https://doi.org/10.1016/j.ibiod.2023.105599>
- Wan YZ, Huang Y, Yuan CD, Raman S, Zhu Y, Jiang HJ, He F, Gao C (2007) Biomimetic synthesis of hydroxyapatite/bacterial cellulose nanocomposites for biomedical applications. *Mater Sci Eng C* 27(4):855–864. <https://doi.org/10.1016/j.msec.2006.10.002>
- Wan Y, Zuo G, Yu F, Huang Y, Ren K, Luo H (2011) Surface & Coatings technology preparation and mineralization of three-dimensional carbon nano fibers from bacterial cellulose as potential scaffolds for bone tissue engineering. *Surf Coat Technol* 205(8–9):2938–2946. <https://doi.org/10.1016/j.surfcoat.2010.11.006>
- Wang B, Lv X, Chen S, Li Z, Sun X, Feng C, Wang H, Xu Y (2016a) In vitro biodegradability of bacterial cellulose by cellulase in simulated body fluid and compatibility in vivo. *Cellulose* 23:3187–3198. <https://doi.org/10.1007/s10570-016-0993-z>
- Wang X, Zhang Y, Luo J, Xu T, Si C, Oscanoa AJC, Tang D, Zhu L, Wang P, Huang C (2023) Printability of hybridized composite from maleic acid-treated bacterial cellulose with gelatin for bone tissue regeneration. *Adv Compos Hybrid Mater* 6(4):134. <https://doi.org/10.1007/s42114-023-00711-7>
- Wang F, Kim HJ, Park S, Kee CD, Kim SJ, Oh IK (2016b) Bendable and flexible supercapacitor based on polypyrrole-coated bacterial cellulose core-shell composite network. *Compos Sci Technol* 128:33–40. <https://doi.org/10.1016/j.compscitech.2016.03.012>
- Wilson OC Jr, Hull JR (2008) Surface modification of nanophasic hydroxyapatite with chitosan. *Mater Sci Eng C* 28(3):434–437
- Yan C, Sun J, Ding J (2011) Critical areas of cell adhesion on micropatterned surfaces. *Biomater* 32(16):3931–3938. <https://doi.org/10.1016/j.biomaterials.2011.01.078>
- Yang X-Y, Huang C, Guo H-J, Xiong L, Luo J, Wang B, Lin X-Q, Chen X-F, Chen X-D (2016) Bacterial cellulose production from the litchi extract by *Gluconacetobacter xylinus*. *Prep Biochem Biotechnol* 46(1):39–43. <https://doi.org/10.1080/10826068.2014.958163>
- Yin N, Stilwell MD, Santos TMA, Wang H, Weibel DB (2015) Agarose particle-templated porous bacterial cellulose and its application in cartilage growth in vitro. *Acta Biomater* 12(1):129–138. <https://doi.org/10.1016/j.actbio.2014.10.019>

- Yu D, Wang J, Qian K-j, Yu J, Zhu H-y (2020) Effects of nanofibers on mesenchymal stem cells: environmental factors affecting cell adhesion and osteogenic differentiation and their mechanisms. *J Zhejiang Univ Sci B* 21(11):871–884. <https://doi.org/10.1631/jzus.B2000355>
- Zaborowska M, Bodin A, Bäckdahl H, Popp J, Goldstein A, Gatenholm P (2010) Microporous bacterial cellulose as a potential scaffold for bone regeneration. *Acta Biomater* 6(7):2540–2547. <https://doi.org/10.1016/j.actbio.2010.01.004>
- Zhang L, Zhang Q, Zheng Y, He Z, Guan P, He X, Hui L, Dai Y (2018) Study of Schiff base formation between dialdehyde cellulose and proteins, and its application for the deproteinization of crude polysaccharide extracts. *Ind Crops Prod* 112:532–540
- Zhao R, Xie P, Zhang K, Tang Z, Chen X, Zhu X, Fan Y, Yang X, Zhang X (2017) Selective effect of hydroxyapatite nanoparticles on osteoporotic and healthy bone formation correlates with intracellular calcium homeostasis regulation. *Acta Biomater* 59:338–350
- Zhao S, Arnold M, Ma S, Abel RL, Cobb JP, Hansen U, Boughton O (2018) Standardizing compression testing for measuring the stiffness of human bone. *Bone Jt Res* 7(8):524–538
- Zhou H, Lee J (2011) Nanoscale hydroxyapatite particles for bone tissue engineering. *Acta Biomater* 7(7):2769–2781. <https://doi.org/10.1016/j.actbio.2011.03.019>
- Zhu Q, Chen X, Liu Z, Li Z, Li D, Yan H, Lin Q (2023) Development of alginate-chitosan composite scaffold incorporation of bacterial cellulose for bone tissue engineering. *Int J Polym Mater Polym Biomater* 72(4):296–307. <https://doi.org/10.1080/00914>

**Publisher's Note** Springer Nature remains neutral with regard to jurisdictional claims in published maps and institutional affiliations.